

# Microstructure and Properties of Aluminum Alloy 2090 Weldments

### *Weld properties are correlated to the effects that EBW and GTAW have on microstructure formation*

BY A. J. SUNWOO AND J. W. MORRIS, Jr.

**ABSTRACT.** The effects of welding on aluminum alloy 2090 are examined along with the metallurgical changes associated with welding and aging. The results of the study show that the gas tungsten arc (GTA) and electron beam (EB) weldment properties are controlled by the precipitate size and distribution. There is a tradeoff between strength and elongation. In the as-welded condition, solid solution strengthening is the primary strengthening mechanism present. As a result, the weldment strengths are less than 200 MPa (29 ksi), but the elongations are greater than 4%. In the postweld aged condition, an inhomogeneous distribution of solutes results in an inhomogeneous distribution of precipitates, causing strain localization. Although the weldment strengths increase, the weldment elongations decrease precipitously. The peak strengths of EB and GTA weldments are obtained aging at 160°C (320°F) for 32 h with 75% joint efficiency and at 190°C (374°F) for 16 h with 65% joint efficiency, respectively. Aging at 230°C (446°F) leads to coarsening of precipitates as well as the intermetallic constituents; the weldment strengths deteriorate rapidly, but the elongations improve. The best overall weldment properties are obtained in the solution heat treated and aged conditions, and are associated with a homogeneous distribution of strengthening precipitates.

## Introduction

A material's properties are determined by its composition and microstructure. In turn, microstructure is determined by composition and processing. For aluminum alloy (AA) 2090-T8E41, the right blend of chemical composition and thermal-mechanical processing produced a microstructure, that, combined with its composition, resulted in properties that are equivalent or superior to current commercially available high-strength aluminum alloys at room and cryogenic temperatures, respectively (Refs. 1-5). AA 2090, with a combination of high

specific strength and toughness, and high specific modulus, is a promising material for the weight-limited cryogenic structures. However, for some cryogenic applications, welding is required.

The weld properties are determined by the same factors as the base metal properties: microstructure and composition. During welding, a localized region of the base metal is melted and resolidified. The fusion zone morphology, as well as the solute distribution, depend on the constitutional undercooling of the individual process. Hence, different welding processes affect the weld properties differently. The objective of this research is to examine the effects of welding processes, with overall composition held constant, on the microstructure and solute segregation, and to correlate its effects to the weldment properties. In addition, the weldment aging responses are also examined.

## Experimental Procedure

The chemical composition of as-received 2090 in wt-% is 3.0Cu-2.2Li-0.12Zr-Al. The as-received 2090 sheet was in the T3 temper (solution heat treated and stretched 4.6%). The sheet was cut into weld coupons of 102 × 203 mm (4 × 8 in.). The weld coupons were machined from their initial thickness of 4.3 mm (0.17 in.) to approximately 3.2 mm (0.12 in.) in order to remove distort-

tion and processing oxide. Prior to welding, the weld coupons were chemically cleaned using 5 vol-% sodium hydroxide in water, followed by concentrated nitric acid.

The two welding processes chosen for this study were gas tungsten arc (GTA) and electron beam (EB) welding. These processes were used to produce a significant difference in the as-solidified microstructure and solute segregation. The welding parameters for GTAW and EBW are listed in Table 1. Autogenous, bead-on-plate welds were produced transverse to the rolling direction. For GTA welding, direct current electrode negative (DCEN) (straight polarity) was used, and welding was conducted on a water-cooled chill block in an argon atmosphere. These precautions, mechanical and chemical cleaning, welding in an inert atmosphere, and use of a water-cooled chill block, were taken to prevent porosity and hot cracking.

The base metal of T3 temper and as-welded weldments were aged at 160°, 190°, and 230°C, to the peak-aged condition. In addition to the postweld aged conditions, the solution-heat-treated-and-aged (SHTA) conditions of the base metal and both EB and GTA weldments were also investigated. The optimum temperatures for SHT were determined using differential scanning calorimetry. The SHTA process consists of a three-step heat treatment: 535°C (995°F) for 15 min, 550°C (1022°F) for 15 min, water quench, and subsequent aging at 160°C. Figure 1 shows the tensile specimen configurations. The overall specimen size was 89 mm (3.5 in.) with

## KEY WORDS

2090 Al-Cu-Li Alloy  
Weldability/Aging  
Electron Beam Weld  
Gas Tungsten Arc Weld  
Aging Temperature  
Joint Efficiency  
Hot Cracking  
Grain Size Effects  
Solution Heat Treat  
Fractography

*A. J. SUNWOO and J. W. MORRIS, Jr., are with the Center for Advanced Materials Lawrence Berkeley Laboratory and the Department of Materials Science and Engineering, University of California, Berkeley, Calif.*

*Based on paper presented at the 69th Annual AWS Meeting, held April 17-22, 1988, in New Orleans, La.*









### Mechanical Properties

The yield strengths, ultimate tensile strengths (UTS), and elongations of base metals, EB weldments, and GTA weldments are presented in Table 2. The results of the aging study indicated that 2090 strength degraded after exposure to temperatures greater than 200°C. The best overall strength and elongation combination for the base metal followed aging at 160°C for 32 h. The base metal peak-aged at 190°C for 16 h showed an insignificant improvement in strength, but had higher elongation. However, specimens aged at 230°C for 4 and 16 h were severely overaged; the yield strengths of the specimens aged for 16 h decreased to less than 50% of the 160°C peak-aged condition, and elongation had lowest value of all aging conditions.

For EB weldments, the highest strengths were obtained by aging at 160°C for approximately 32 h. The aging response of the EB weldments was similar to that of the base metal when aged at 190°C and at 230°C. As the aging temperature increased, the peak strength was achieved in a shorter time, as expected. However, the peak yield strength at 160°C was higher than that of 190°C. The EB weldments also became overaged at 230°C.

Higher yield strength was achieved for GTA weldments aged at 190°C than at 160°C. The peak yield strength at 190°C was reached between 16 and 24 h, while the yield strength of weldments aged at 160°C continued to increase and peaked beyond 32 h. Aging at 230°C also adversely affected GTA weldment properties. The joint efficiencies of EB and GTA weldments in the near peak-aged condition were 75% and 65%, respec-



Fig. 5—TEM bright field image of a solution heat treated and aged GTA fusion zone; near [211] orientation

tively.

As the weldment strength increased with aging, the weldment elongation decreased precipitously—Table 2. In the as-welded condition the weldment elongations were greater than 4%. In the peak-aged condition, the elongations were less than 1%. Visual observation of

the tested as-welded EBW and GTAW specimens revealed localized deformation in the fusion zone and minimal deformation in other areas. In the tested peak-aged weldments, there was no evidence of deformation in the fusion zone. In the overaged condition, the weldment elongation improved slightly. It is noteworthy

### Table 2—Tensile Test Results

Heat Treatment (°C/h)	EBW/GTAW/BM 0.2% Yield Strength (MPa)	EBW/GTAW/BM UTS <sup>(a)</sup> (MPa)	EBW/GTAW/BM Total Elongation (%)
T3; As-welded	195/175/281	288/270/352	4.4/4.4/9.3
PWA <sup>(b)</sup>			
160/8	359/253/517	407 <sup>(a)</sup> /326 <sup>(a)</sup> /592	0.6/1.2/8.9
160/16	— /295/560	— /314 <sup>(a)</sup> /605	— /0.8/9.4
160/32	438/314/574	445 <sup>(a)</sup> /372 <sup>(a)</sup> /608	0.3/0.8/9.4
190/2	— / — / —	401 <sup>(a)</sup> / — / —	0.1/ — / —
190/4	357/291/493	380 <sup>(a)</sup> /350 <sup>(a)</sup> /538	0.5/0.7/8.8
190/16	350/334/496	363 <sup>(a)</sup> /371 <sup>(a)</sup> /547	0.3/0.5/11.2
190/24	— /325/ —	— /363 <sup>(a)</sup> / —	— /0.5/ —
230/2	— /230/ —	— /288/ —	— /1.2/ —
230/4	314/259/338	354 <sup>(a)</sup> /320 <sup>(a)</sup> /416	0.7/1.0/11.0
230/16	274/248/279	321 <sup>(a)</sup> 300 <sup>(a)</sup> /371	1.3/1.2/7.8
SHT A <sup>(c)</sup>			
160/4	311/315/313	415 <sup>(a)</sup> /396 <sup>(a)</sup> /403 <sup>(a)</sup>	5.4/2.5/6.9
160/16	416/384/413	479 <sup>(a)</sup> /435 <sup>(a)</sup> /485 <sup>(a)</sup>	1.8/1.1/10.1
All weld metal <sup>(d)</sup>			
As-welded	— /137/ —	— /250/ —	— /17.0/ —
160/32	— /254/ —	— /322/ —	— /1.5/ —

(a) Fracture strength.

(b) PWA = postweld aged.

(c) SHT&A = solution heat treated and aged after welding.

(d) See Fig. 1B.







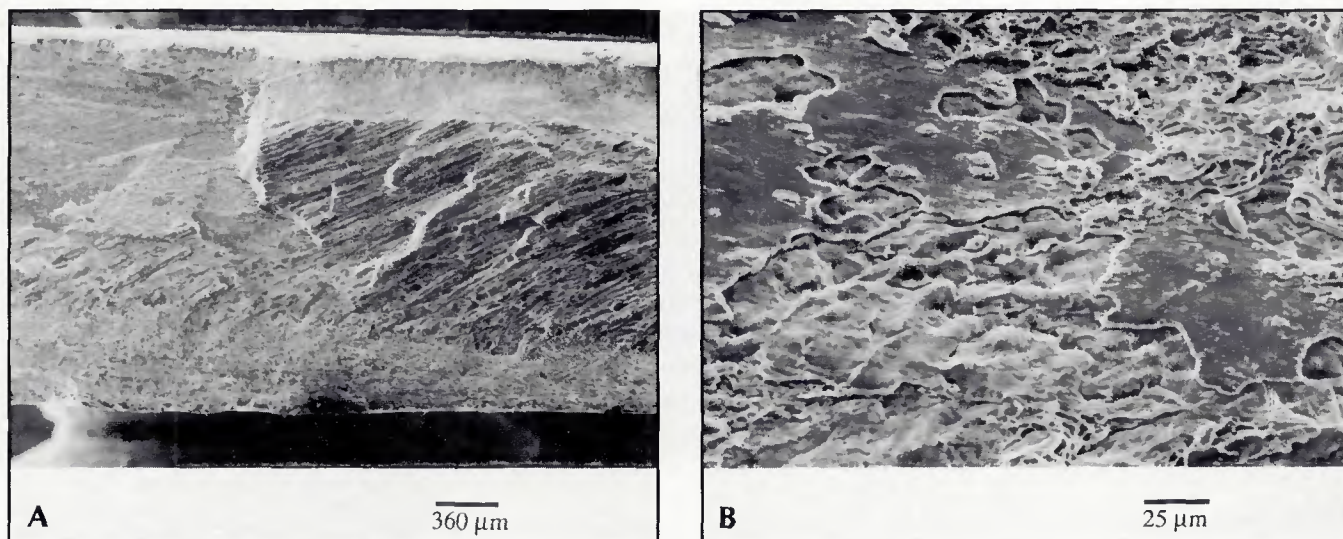


Fig. 9—SEM fractographs of GTA weldment in solution heat treated and aged at 160°C for 4 h. A—Overall fracture surface; B—partially melted region

ary cracks at the dendrite boundaries. Failure occurred close to the center of the fusion zone. Figure 8 shows the SEM fractographs of the as-welded, peak-aged, and overaged conditions. The as-welded GTA fracture surface was similar to the as-welded EB fracture surface with void formation and slip evident along the dendrite boundaries—Fig. 8A. In the peak-aged condition, spherical intermetallic phases decorated the dendrite boundaries, and in the overaged condition, these phases became globular, as shown in Figs. 8B and 8C. Figure 9 shows the GTA specimen fracture surface after SHTA for 4 h. There were three distinct regions: the lamellar microstructure of base metal, the dendritic microstructure of the weld, and the partially melted region (PMR) of the HAZ—Fig. 9A. Figure 9B shows the PMR, identified by its smooth surface decorated with various size particles. The PMR was also present on the other fracture surfaces of SHTA GTA weldments. Fracture may have initiated at the PMR regions, resulting in a premature failure.

## Discussion

### Effect of Grain Size

The grain size is known to influence the strength of an alloy. However, for the range of grain sizes considered, the influence of grain size on strength is found to be small. In general, the grain size dependence on the strength can be predicted using the Hall-Petch relationship (Ref. 9). The average grain size of the GTA fusion zone is 150  $\mu\text{m}$ , while the average grain size of the base metal in the longitudinal direction is an order of magnitude larger. Assuming that the SHT produced a homogeneous distribution of solutes in the GTA weldments and erased prior

thermal mechanical processing (TMP) of the base metal, the effect of grain size on strength is compared for the SHTA conditions—Table 2. Qualitatively, the GTA weldment is expected to be stronger. However, equivalent yield strengths are found for the GTA weldments and the base metal aged at 160°C for 4 h. With a continuous aging, the yield strength of the GTA weldments is approximately 30 MPa (4.3 ksi) lower than that of base metal. This indicates that there are other metallurgical factors contributing to the properties. Thus, the grain size has a limited influence on the strength of the alloy.

### Effect of Solute and Precipitate Strengthening

The differences in base metal properties and weldment properties can be explained by their solute/precipitate distribution. For the base metal, TMP is utilized to attain a homogeneous distribution of solutes and to control the formation and distribution of the strengthening phases during aging. By influencing precipitation behavior, a combination of high strength and toughness is obtained. The major strengthening phases in 2090 are the plate-like  $T_1$  and  $\theta'$  precipitates.

Prior TMP effects are almost erased in the fusion zone of the weldments. Instead, the degree of solute segregation is established during welding. The EBW fusion zone shows more limited solute segregation than that of the GTAW fusion zone. This distinct difference between the EB and GTA fusion zones affects the solid solution strengthening and aging response and, in turn, the weldment properties.

In the as-welded condition, there is a limited strengthening precipitate in the fusion zone, and hence, the primary

strengthening mechanism is solid solution strengthening. When the effects of solid solution strengthening on the yield strengths of as-welded EB and GTA weldments are compared, the difference in yield strengths is only 20 MPa. When the near peak-aged yield strengths of EB and GTA weldments are compared, the difference in strengths is at least 100 MPa (14.5 ksi). Similarly, when yield strengths of the GTA weldments postweld aged at 160°C for 16 h and SHTA aged at 160°C for 16 h are compared, the yield strength of the SHTA weldments is 90 MPa (13 ksi) higher. These comparisons indicate that the precipitate strengthening mechanism is a more effective strengthening mechanism than solid solution strengthening in the fusion zone. Also, a homogeneous distribution of solutes, which leads to a more homogeneous distribution of precipitates, is important for the aged properties.

The weldment strength and elongation are inversely related and are closely tied to the tensile failure mode. Since solid solution strengthening is the only strengthening mechanism of significance present in the as-welded condition, dislocation motion is less effectively impeded than if strengthening precipitates are present. As a result, the weldment elongation is greater than 4%, and the failure mode is ductile fracture. In the postweld aged condition, due to inhomogeneous distribution of the precipitates, strain is localized near the dendrite boundaries and subsequently leads to interdendritic failure (Refs. 10, 11). As the weldment becomes overaged, the precipitates as well as the intermetallic phases are coarsened (Ref. 12, 13). The distribution of the precipitates becomes nonuniform within the dendrite, and the primary strengthening mechanism becomes less effective. Thus, the dislocation movement be-



comes easier and the elongation improves slightly. By homogenizing the solute/precipitate distribution, both strength and elongation are improved. In the SHT and underaged condition, the precipitate size has not been optimized and hence, the dislocation movement is not as effectively impeded, leading to lower strength and higher elongation. However, at longer aging times, a precipitate-free zone has formed adjacent to the dendrite boundary intermetallic phases, especially in the EB fusion zones. Since PFZ is softer than other areas, a localized strain develops and causes interdendritic ductile fracture (Ref. 10, 12).

## Conclusions

The effects of welding on AA 2090 were studied along with the metallurgical changes associated with welding and aging. The weldment properties are controlled by the precipitate size and distribution. There is a tradeoff between strength and elongation. The following specific conclusions are drawn.

1) In the as-welded condition, solid solution strengthening is the primary strengthening mechanism present. As a result, the weldment strengths are less than 200 MPa, but the elongations are greater than 4%.

2) In the postwelded aged condition, an inhomogeneous distribution of solutes results in an inhomogeneous distribution

of precipitates, causing strain localization. Although the weldment strengths increase, the weldment elongations decrease precipitously.

3) The highest peak yield strengths of EB and GTA weldments are obtained at 160°C for 32 h with 75% joint efficiency and at 190°C for 16 h with 65% joint efficiency, respectively. Aging at 230°C leads to coarsening of precipitates, as well as the intermetallic constituents. As a result, weldment strengths deteriorate rapidly and elongations improve.

4) The best overall weldment properties are obtained in the solution heat treated and aged conditions, due to a homogeneous distribution of strengthening precipitates.

### Acknowledgments

The authors would like to thank the Aluminum Company of America for providing the material and B. Olsen of the Lawrence Livermore National Laboratory for producing the EB welds. This work is supported by the Director, Office of Energy Research, Office of Fusion Energy, Development and Technology Division of the U.S. Department of Energy under contract #DE-AC03-76SF00098.

## References

1. Glazer, J., Verzasconi, S. L., Dalder, E. N. C., Yu, W., Emigh, R. A., Ritchie, R. O., and Morris, J. W. 1986. *Adv. Cryo. Eng.* 32:397-404.

2. Glazer, J., Verzasconi, S. L., Sawtell, R. R., and Morris, J. W. 1986. *Metall. Trans.*, 18A: 1695 to 1701.
3. Rioja, R. J., Bretz, P. E., Sawtell, R. R., Hunt, W. H., and Ludwiczak, E. A., 1983. *Aluminum Alloys II*. Conf. Proc., eds. E. A. Starke, Jr., and T. H. Sanders, Jr., pp. 1781-1797. The Metallurgical Society of AIME.
4. Staley, J. T., Rioja, R. J., Wyss, R. K., and Liu, J. 1987. Alcoa ALTC Division Report, 04-87-JD-34-56.
5. Ashton, R. F., Thompson, D. S., Starke, Jr., E. A., and Lin, F. S. 1986. *Aluminum-Lithium Alloys III*. Conf. Proc., eds. C. Baker, P. J. Gregson, S. J. Harris, and C. J. Peel, pp. 66-77. The Institute of Metals, London, England.
6. Tosten, M. H., Vasudevan, A. K., and Howell, P. R. 1986. *Aluminum-Lithium Alloys III*. Conf. Proc. eds. C. Baker, P. J. Gregson, S. J. Harris, and C. J. Peel, pp. 490-495. The Institute of Metals, London, England.
7. Rioja, R. J., and Ludwiczak, E. A. 1985. *Aluminum-Lithium Alloys III*. Conf. Proc., eds. C. Baker, P. J. Gregson, S. J. Harris, and C. J. Peel, pp. 471-482. The Institute of Metals, London, England.
8. Toston, M. H., Vasudevan, A. K., and Howell, P. R. 1986. *Aluminum-Lithium Alloys III*. Conf. Proc., eds. C. Baker, P. J. Gregson, S. J. Harris, and C. J. Peel, pp. 483-489. The Institute of Metals, London, England.
9. Dollar, M., and Thompson, A. W. 1987. *Acta Metall.* 35 (1):227-235.
10. Vasudevan, A. K., and Doherty, R. D. 1987. *Acta Metall.* 35 (6):1193-1219.
11. Gräf, M., and Hornbogen, E. 1977. *Acta Metall.* 25:883-889.
12. Thomas, G., and Nutting, J. 1959. *Journal of Institute of Metall.* 88:81-90.
13. Nicholson, R. B., Thomas, G., and Nutting, J. 1958. *Journal of Institute of Metals.* 87:429-438.

WRC Bulletin 331  
February 1988

This Bulletin contains two reports prepared by the Japan Pressure Vessel Research Council (JPVRC) Subcommittee on Pressure Vessel Steels. The reports are involved with the variation in toughness data for weldments in pressure vessel steel structures.

## Metallurgical Investigation on the Scatter of Toughness in the Weldment of Pressure Vessel Steels—Part I: Current Cooperative Research

This report covers the background of current cooperative research from 1973 to the present, covering 137 references on toughness and toughness testing of weldments.

## Metallurgical Investigation on the Scatter of Toughness in the Weldment of Pressure Vessel Steels—Part II: Cooperative Research

The objective of this report was to investigate the variation in toughness of multipass weldments in a welded joint.

Publication of these reports was sponsored by the Subcommittee on Thermal and Mechanical Effects on Materials of the Welding Research Council. The price of WRC Bulletin 331 is \$28.00 per copy, plus \$5.00 for postage and handling. Orders should be sent with payment to the Welding Research Council, 345 E. 47th St., Suite 1301, New York, NY 10017.